

Virtual Laboratory for Technology FES FY2017 Third Quarter Report

Phil Ferguson
for the VLT members



Director's Corner

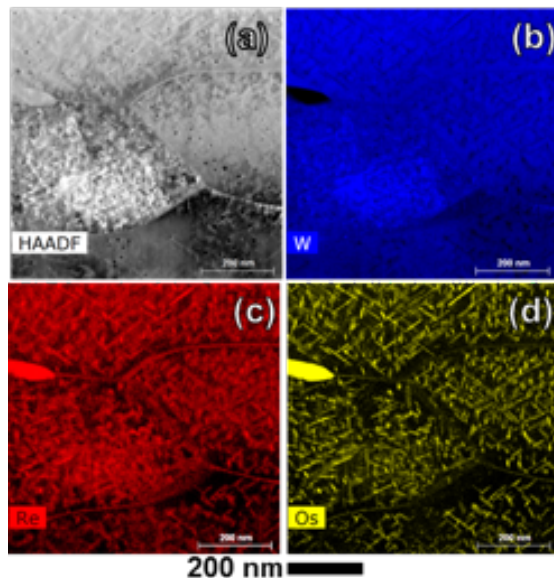
- Bi-monthly teleconferences are continuing with good representation. Additional teleconferences are held as needed to prepare for whitepaper submissions, presentation discussions, etc.
- The VLT participated in the FY19 FES budget planning discussions. This was a new activity for the VLT and we hope that the information provided and discussions held were useful to our program managers.
- The VLT members continue to participate in/contribute to both the National Academies Study and the FESAC Transformative Enabling Capabilities Subcommittee activities.
 - The VLT exhibited outstanding response to the whitepaper calls - by rough estimates, over half of the whitepapers/presentations for the FESAC subcommittee and just under 40% of the community whitepapers submitted were from the VLT or on VLT related topics.
- This and future highlights will continue to cover research highlights from recent VLT publications and the main VLT research areas:
 - Magnet Systems; Heating & Current Drive; Plasma Fueling/ ELM Pacing/Disruption Mitigation
 - Plasma Facing Components; Plasma Materials Interactions; Structural Materials
 - Design/Systems studies; Power Handling; Fusion Safety; Fuel Cycle Research; Blanket Technology; Vacuum System
 - ***In Q3: We are also presenting a number of highlights from the Young/Fresh Faces of the VLT***

If you have any questions on the information in this report, please don't hesitate to contact us.

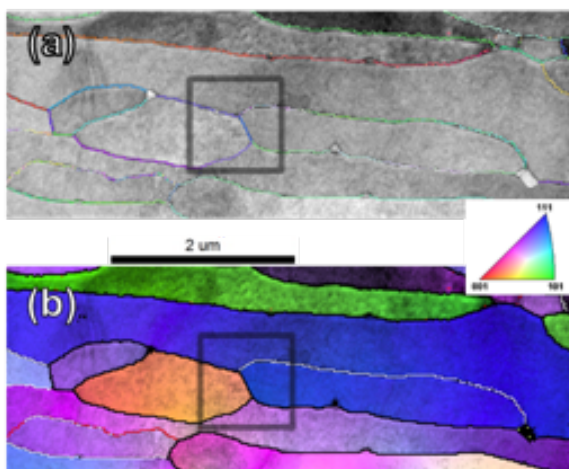
Nanoscale Characterization of Neutron-Irradiated Tungsten May Lead to Improved Material

Research Highlight

Characterization



(a) STEM image and (b-d) STEM X-ray maps show significant precipitation (Re,Os) and grain boundary segregation (mostly Re).



tKD image quality (a) showing grain boundary misorientation axes, and (b) grain orientation map showing grain boundary angle (white: $<5^\circ$, red, 5-15°; black, $>15^\circ$). The gray square denotes the region of the STEM data above.

Scientific Achievement

Understanding structural evolution in nuclear materials requires high-resolution, high-sensitivity probes of the chemistry and crystallography of the post-irradiation state. We demonstrate the correlation of transmission Kikuchi diffraction (tKD) crystallography with scanning transmission electron microscopy (STEM) X-ray chemical mapping of grain boundaries in order to perform correlative measurements.

Significance and Impact

Irradiated tungsten suffers radiation-induced precipitation and segregation (RIP and RIS), especially at grain boundaries. This combined method allows measurements of RIS and RIP as a function of grain boundary character.

Research Details

3 dpa, $\sim 800^\circ\text{C}$ HFIR-irradiated polycrystalline tungsten was prepared via focused ion beam (FIB) and measured using tKD in SEM and X-ray mapping in STEM.

Application

Determination of RIS and RIP as a function of grain boundary character may enable grain-boundary engineering to minimize degradation under irradiation.

C.M. Parish, K. Wang, and P. D. Edmondson, Viewpoint: Nanoscale chemistry and crystallography are both the obstacle and pathway to advanced radiation-tolerant materials, *Scripta Materialia*, (in press) (Early Career Award research program)



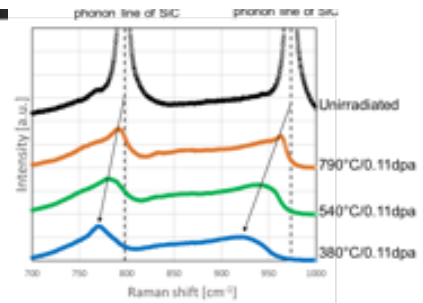
Fundamental Measurements of Defects in SiC Guide Development of Improved Composites for Fusion

Research Highlight

Raman spectroscopy characterizes atomistic scale lattice disorder



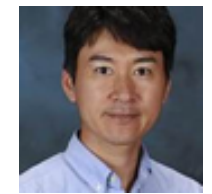
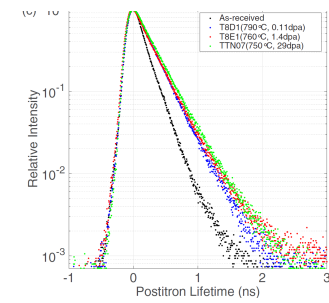
T. Koyanagi, M. J. Lance, and Y. Katoh. "Quantification of irradiation defects in beta-silicon carbide using Raman spectroscopy." *Scripta Materialia* 125 (2016): 58-62.



Positron annihilation spectroscopy reveals the nature of vacancy defects



X. Hu, T. Koyanagi, Y. Katoh, and B. D. Wirth. "Positron annihilation spectroscopy investigation of vacancy defects in neutron-irradiated 3C-SiC." *PHYSICAL REVIEW B* 95, 104103 (2017)



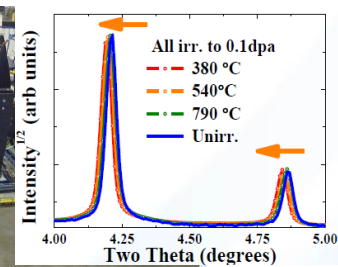
Takaaki Koyanagi
Early Career Staff

These defect properties combined with computational modeling help understand microstructural evolution and property changes

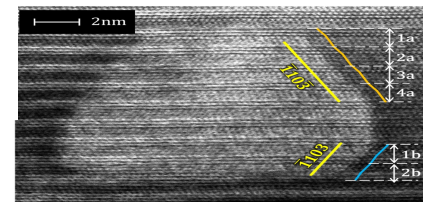
High-energy X ray diffraction establishes long range lattice disorder



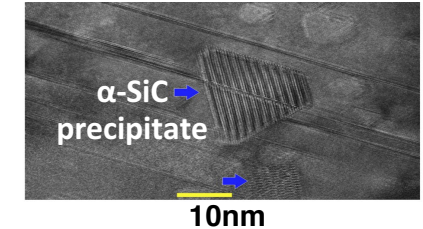
D. J. Sprouster, T. Koyanagi, E. Dooryhee, S. K. Ghose, Y. Katoh, and L. E. Ecker. "Microstructural evolution of neutron irradiated 3C-SiC" *Scripta Materialia* 137 (2017) 132-136



High-resolution transmission electron microscopy identifies defect nanostructure



S. Kondo, C. M. Parish, T. Koyanagi, and Y. Katoh, "Equilibrium shapes and surface selection of nanostructures in 6H-SiC." *APPLIED PHYSICS LETTERS* 110, (2017) 142106.



C. M. Parish, T. Koyanagi, S. Kondo, and Y. Katoh, "Irradiation-induced β to α SiC transformation at low temperature." *Scientific Reports* 7 (2017) 1198

Progress on early stage growth of nanostructured tungsten from implanted low energy helium

Intermediate flux ion source used to study fuzz formation

- Thickness by FIB profiling and He ion microscopy comparable to other experiments (TJ Petty et. al., *Nucl Fusion*)
 - Fluence: $5 \times 10^{23} - 1.2 \times 10^{25} \text{ He m}^{-2}$; Energy: 75 eV
 - Covers morphologies from initial grooves and holes to fully developed tendrils

Development of new surface morphology tools

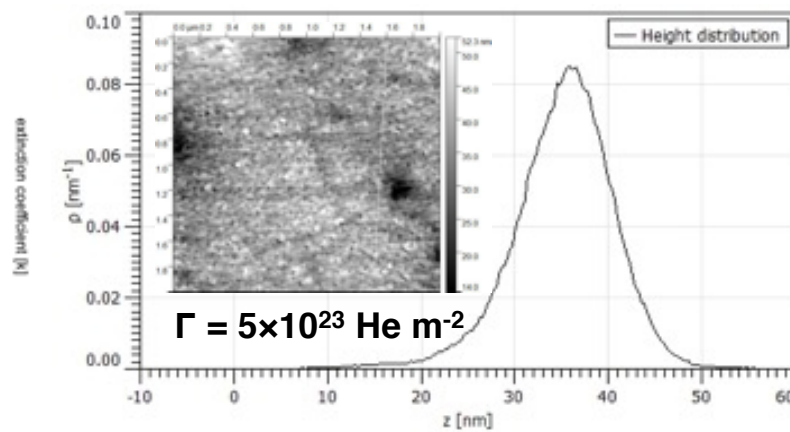
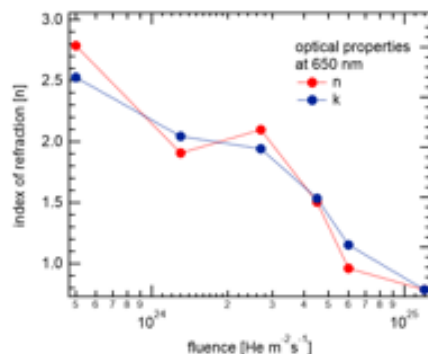
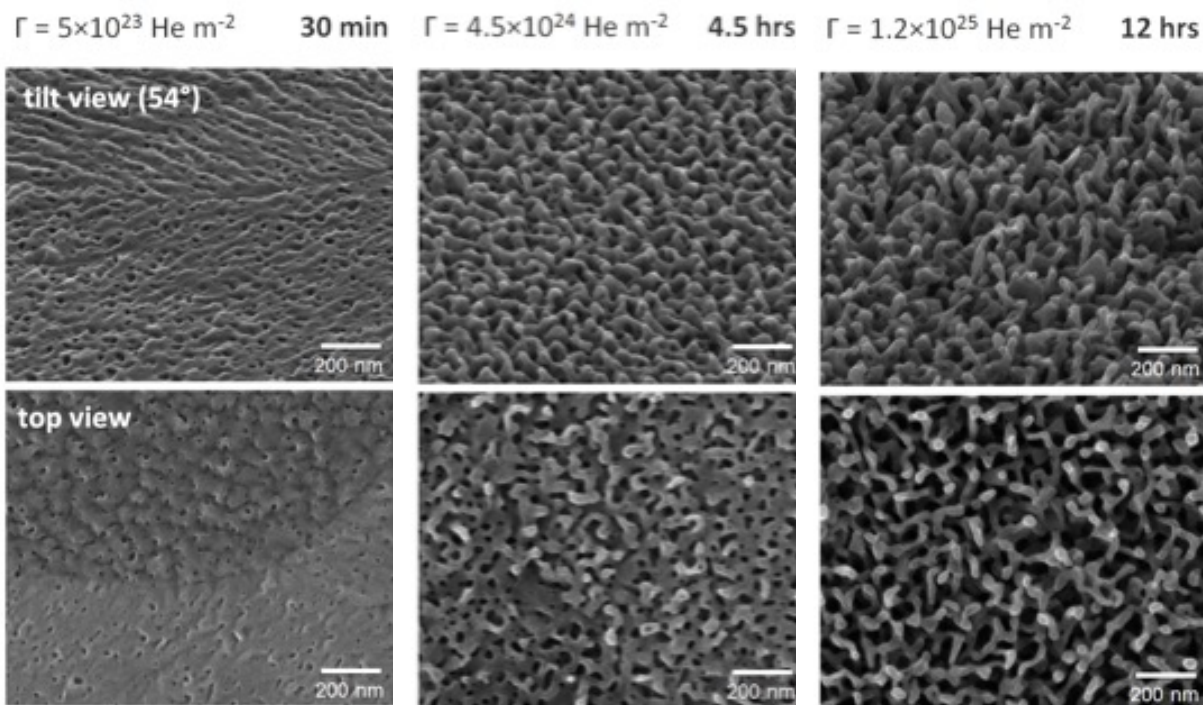
- Spectroscopic ellipsometry shows high correlation

Comparison with theory

- AFM and continuum model development at UT (B. Wirth)



Robert Kolasinski, SNL
Early Career Project

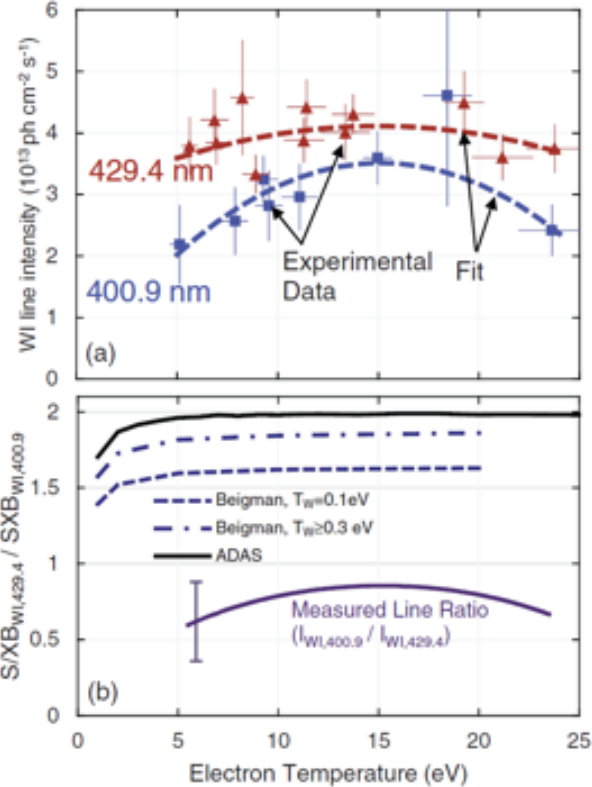


Unraveling complex atomic physics of W to properly diagnose high-Z sourcing via spectroscopy

Scientific Achievement

An electron density dependence was measured for the WI 400.9 nm S/XB coefficient for the first time, important for interpretation of W sourcing during partially detached plasma operation and during ELMs.

The intensity ratio of the WI 400.9 nm line to the 429.4 nm line was measured to be a factor of two lower than theory, necessitating a re-evaluation of the neutral tungsten metastable populations.

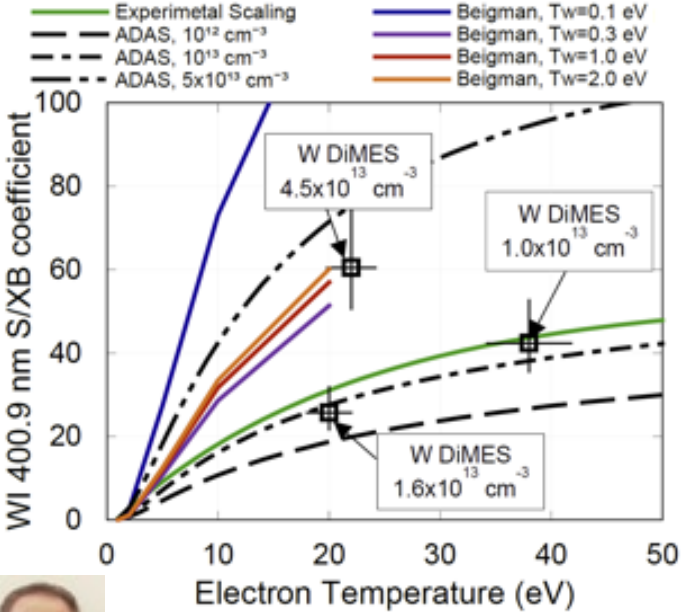


Research Details

- W-coated graphite DiMES samples exposed to well-diagnosed L-mode plasmas in the DIII-D divertor.
- Detailed spectroscopic characterization performed of the WI 400.9 nm line and the WI 429.4 nm line, including absolute intensity calibration.
- Photon emission rates compared to post-mortem RBS measurements of gross erosion to determine ionization per photon (S/XB) coefficients.
- Line intensity ratios and S/XB values were compared to two theoretical data sets (Beigman et al. PPCF 2007 and Brezinsek et al., APiP 2013)

Significance and Impact

The first step in the high-Z impurity pathway is the divertor source and thus diagnosing W divertor erosion in H-mode is a crucial issue for ITER. W sources are proportional to the S/XB coefficients, so accurate characterization of this parameter aids in an understanding of how much W erosion can be expected in ITER.



Tyler Abrams: Early Career Staff
 T. Abrams et al., Nucl. Fusion 57 (2017) 056034
 T. Abrams et al., IEEE-TPS (2017) submitted

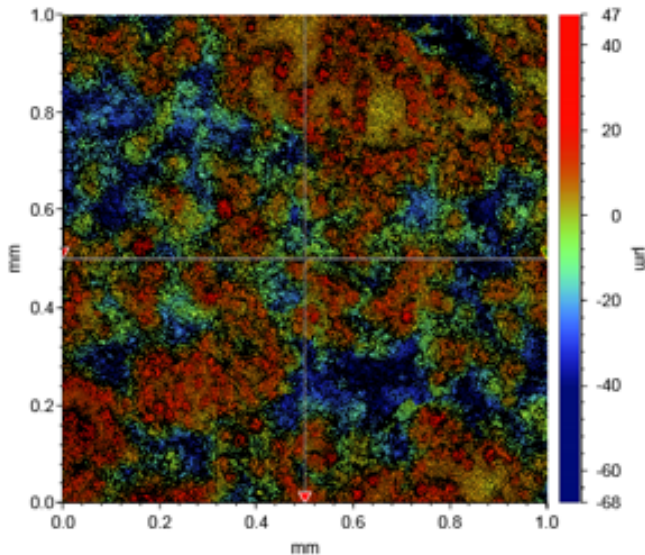
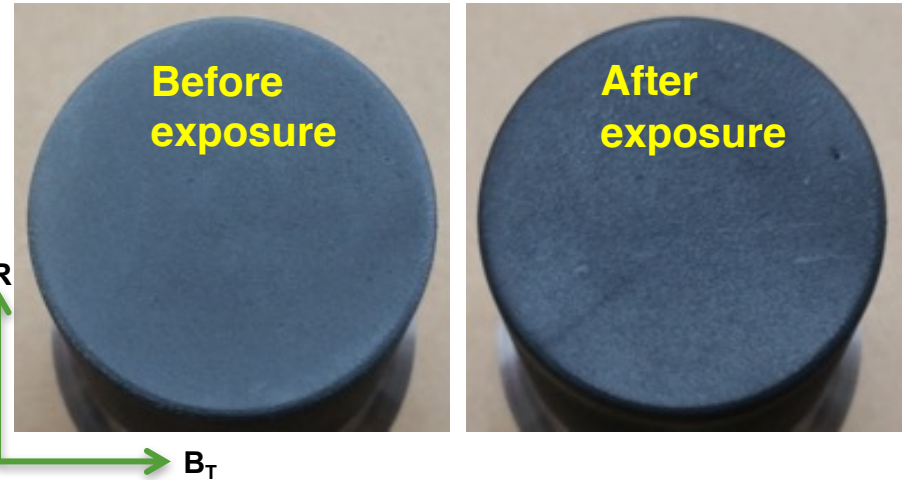
Silicon carbide (SiC) coatings prove to be robust under tokamak divertor level heat fluxes

Scientific Achievement

Silicon carbide coatings formed via CVD were exposed to high divertor heat fluxes in the DIII-D tokamak and exhibited minimal changes in surface morphology and no macroscopic delamination.

Significance and Impact

Silicon carbide is a leading option as a plasma facing material due to its neutron damage resistance, low activation, and low T permeation, but limited testing has been performed on tokamaks. These tests indicate, for the first time, the resilience of SiC coatings to divertor-level heat fluxes without any noticeable changes in surface roughness or flaking/delamination.



Map of SiC DiMES surface morphology after plasma exposure

$R_{RMS, before} = 12.9 \mu m$
 $R_{RMS, after} = 13.5 \mu m$



Tyler Abrams
Early Career Staff

Research Details

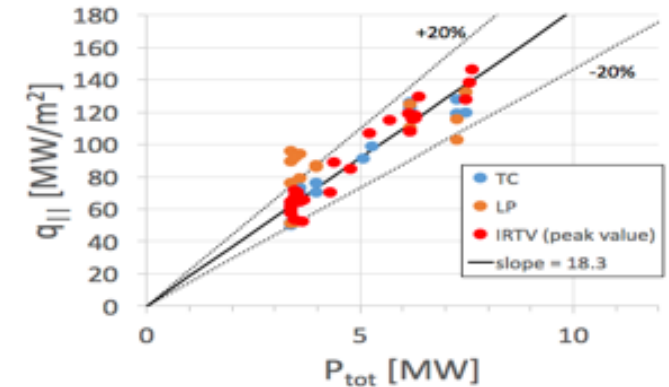
- SiC-coated graphite DiMES sample inserted for ~20 DIII-D H-mode discharges (80 s H-mode exposure).
- Sample exposed to steady state heat fluxes of ~3 MW m⁻² with many transients (ELMs) exceeding 10 MW m⁻² and ~5x10²³ m⁻² of total ion fluence.
- Numerous Si I,II and C II,III lines observed, indicating presence of Si and C erosion.
- Pre- and post-mortem surface profilometry indicates minimal changes in SiC surface roughness before/after plasma exposure.

T. Abrams, S. Bringuier, H. Khalifa, L. Holland
S. Bringuier et al., APS-DPP Conference 2017 (upcoming)

DIII-D heat flux analysis for Small Angle Slot (SAS) divertor with improved measurement capabilities

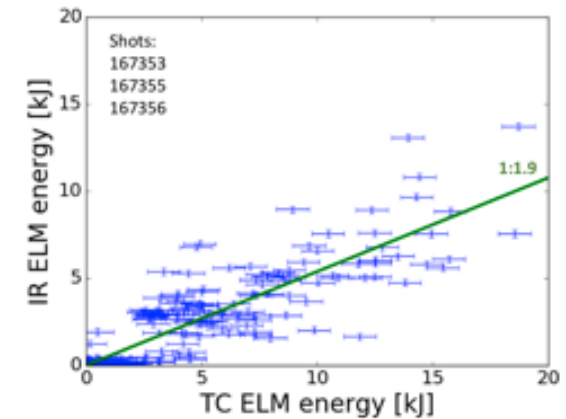
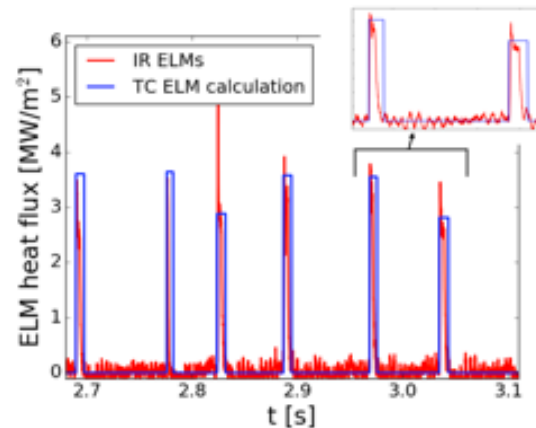
Setting operational specifications

- Average heat flux along B-field vs. total heating power during metal tile campaign
 - Independent measurements from embedded TC's, IRTV, and LPs agree to within 20%
 - Linear extrapolation used for power limits on newly designed SAS Langmuir probes



Improved measurement capabilities

- New technique for obtaining intra-ELM heat flux from embedded TCs
 - Comparison to intra-ELM IRTV deduced heat flux agrees to within ~1.9
 - Technique needed when IRTV camera has no view of the divertor tiles (e.g., SAS divertor configuration) or has limited spatial resolution (e.g., DIMES experiments)

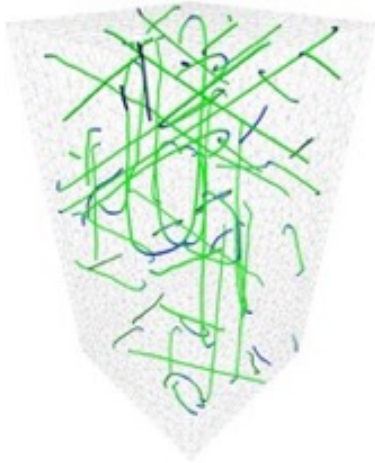


J.L. Barton et. al., "Comparison of heat flux measurement techniques during the DIII-D metal ring campaign," submitted to *Phy. Scr.*

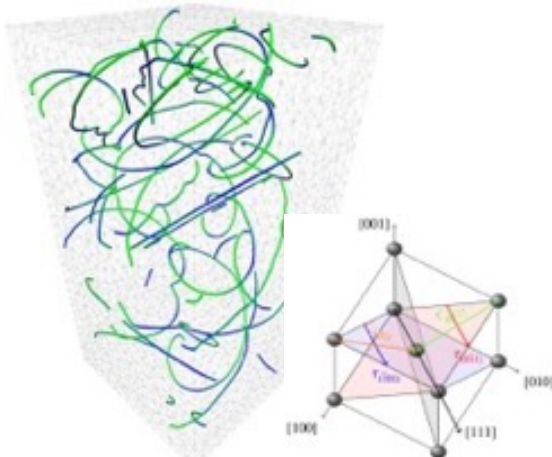
Joseph Barton, postdoc, SNL →



Dislocation Mobility Law Developed for BCC metals



Kink-regime
($\Delta G \geq 0$)



phonon-regime
($\Delta G \leq 0$)

The smooth transition between the kink-regime and the phonon-regime depends on the free energy of kink-pair formation:

$$v(\sigma, T) = \begin{cases} \frac{\tau b}{B(\sigma, T)} \exp\left(-\frac{\Delta G_{kp}(\sigma, T)}{2k_B T}\right) & \text{if } \Delta G_{kp}(\sigma, T) > 0 \\ \frac{\tau b}{B(\sigma, T)} & \text{if } \Delta G_{kp}(\sigma, T) \leq 0 \end{cases}$$

Giacomo Po (Early Carrier Staff), Yanan Cui (Post Doc), David Rivera, David Cereceda, Tom D. Swinburne, Jaime Marian, and Nasr Ghoniem. "A phenomenological dislocation mobility law for bcc metals." *Acta Materialia* **119** (2016): 123-135.

Scientific Achievement

Tungsten and iron are BCC metals. We developed a comprehensive dislocation mobility law that describes the speed of dislocations under any type of stress field and at any temperature. This "mobility law" is the first of its kind.

Significance and Impact

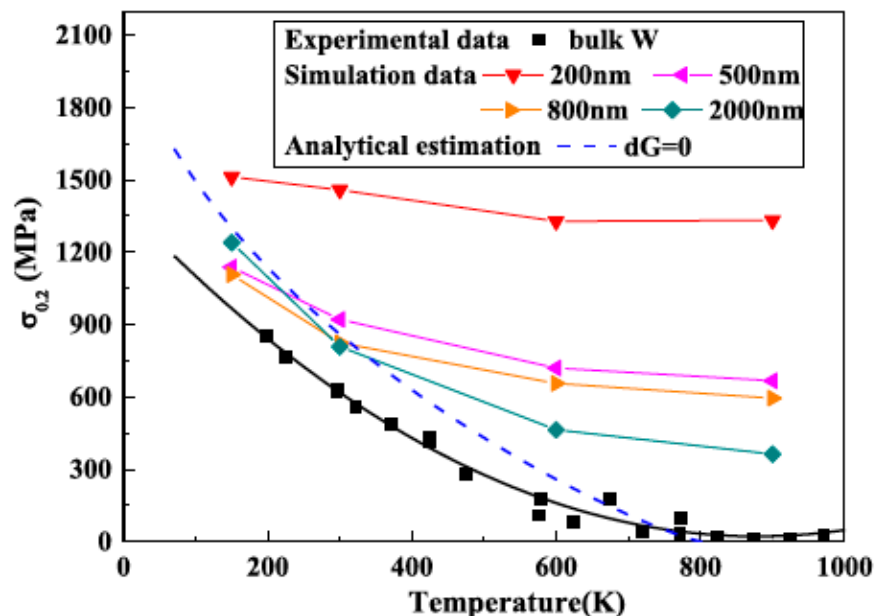
In order to study phenomena like the ductile to brittle transition in bcc metals in DD, a new mobility law has been developed. The law is the most important ingredient in micro- and macro-scale plasticity theories of BCC metals that are based on a description of the materials microstructure.

Research Details

- 1) **Temperature dependence of the flow stress**
 - Due to the fact that the free energy of kink-pair nucleation depends on temperature
 - Flow stress from DD simulations compares well with experimental data
- 2) **Twinning/anti-twinning asymmetry**
 - the flow stress depends on the loading direction;
 - the asymmetry decreases for increasing temperature.
- 3) **Tension/compression asymmetry**
 - the flow stress depends on the sense of the load;
 - the asymmetry decreases for increasing temperature

Temperature insensitivity of the flow stress in body-centered cubic micropillar crystals

Research Highlight



The dependence of the flow (yield) stress on temperature for various sample sizes. Note the insensitivity of the flow stress to test temperature when the sample size is small (e.g. 200 nm).

Yinan Cui (Post Doc), Giacomo Po (Early Career Staff), and Nasr Ghoniem. "Temperature insensitivity of the flow stress in body-centered cubic micropillar crystals." *Acta Materialia* **108** (2016): 128-137.

Scientific Achievement

Plasticity of body-centered cubic (bcc) crystals is known to have a strong dependence on temperature, as a direct consequence of the thermally-activated process of kink pair nucleation and migration with a high energy (Peierls) barrier. Here we demonstrate that, in the sub-micron size scale, such strong temperature dependence of the flow stress must disappear

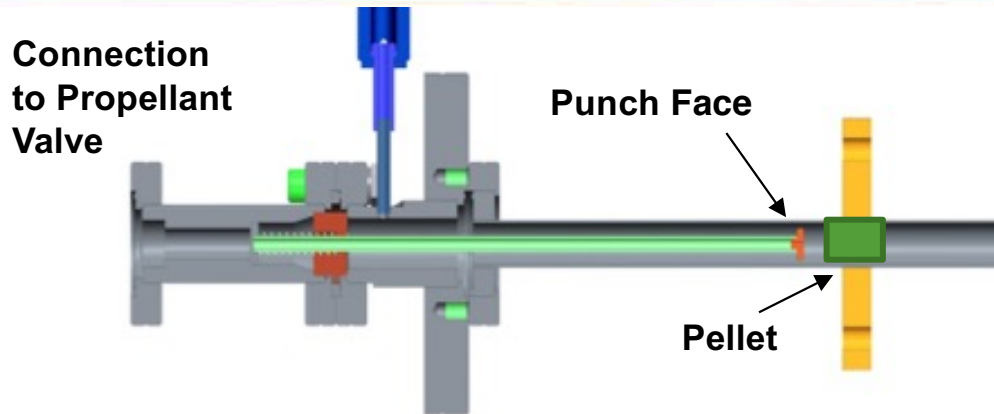
Significance and Impact

This finding opens the door to materials-by-design of nano-grained BCC metals (e.g., tungsten and iron that do not show strong DBTT behavior).

Research Details

Explored the flow stress and hardening behavior of micro-pillar sizes in the range 200-2000 nm at temperatures of 150-900 K. Discrete Dislocation Dynamics (DDD) simulations reveal that weak temperature sensitivity can be rationalized in terms of the weak role of screw dislocations in controlling plasticity; unique to small crystals of finite size. It is shown that finite, sub-micron samples have limited ability to store screw dislocations. The necessity of applying high stress in sub-micron crystals is demonstrated to greatly enhance the mobility of screw dislocations, rendering it close to that of edge dislocations. This leads to a transition of the dislocation mobility mechanism from being thermal-activated kink dominated to being phonon-drag dominated. Thus, the flow stress gradually becomes not governed by the mobility of screw dislocations (as determined by the critical resolved shear stress), giving rise to the weak temperature sensitivity of the flow stress. A dislocation mechanism map in the temperature-size space is proposed to further illustrate this phenomenon in tungsten micropillars.

A prototype punch is able to successfully accelerate 8.5 mm diameter solid argon pellets used for tokamak disruption mitigation



Scientific Achievement

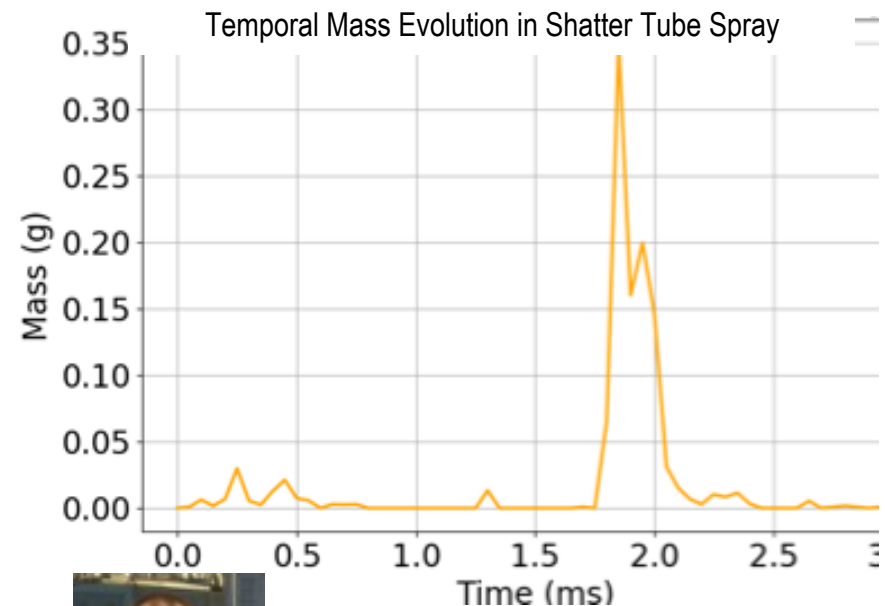
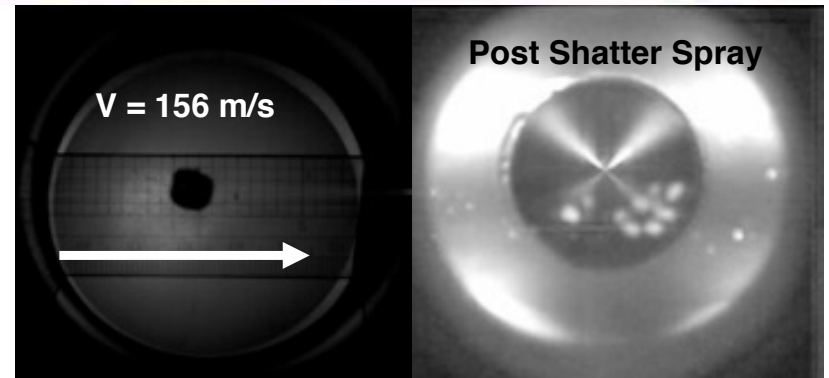
Successfully launched cryogenically frozen argon pellets with a prototype punch to test the DIII-D shatter tube. The punch is needed since the mechanical strength of argon is too great for only a gas gun to dislodge them.

Significance and Impact

Shattered argon pellets are to be used for the dissipation of runaway electrons (REs). The mass temporal evolution in the spray was determined and is crucial for understanding the possible impact on a RE beam. This achievement provides input to the design of the ITER disruption mitigation system.

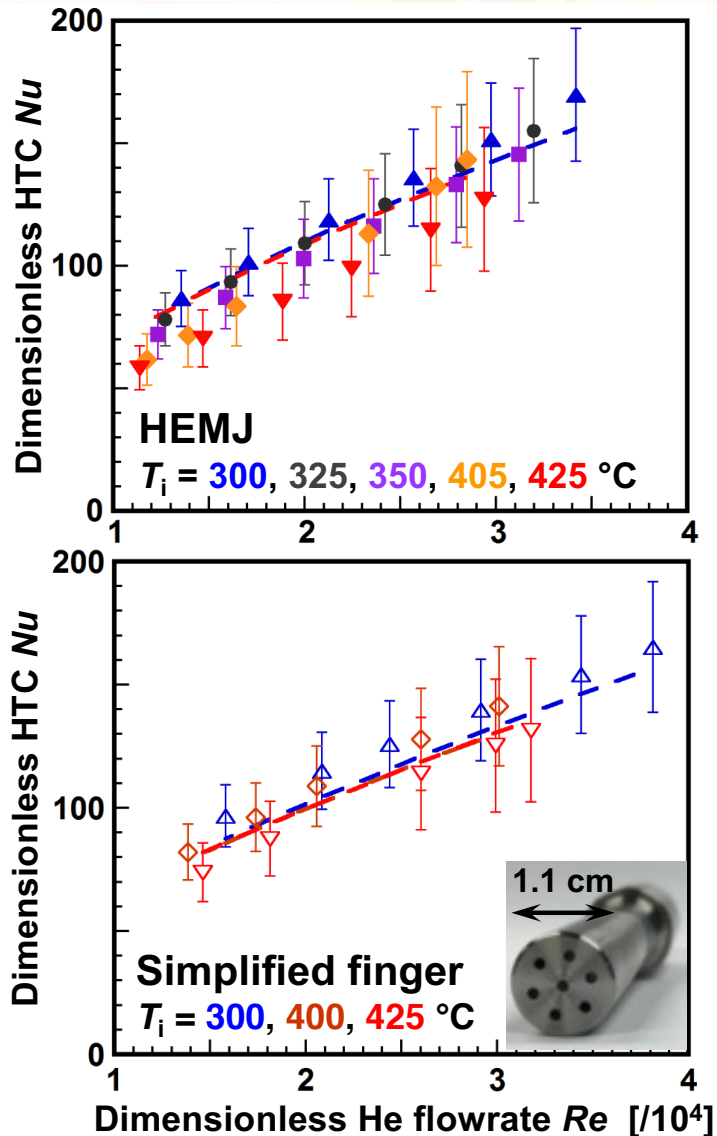
Research Details

The speeds of the pellets ranged from 140 to 210 m/s. They were fired using a fast solenoid valve with ~55 bar of helium propellant gas. Pellets consistently shattered upon impact with the shatter tube. The resulting fragments are ideal for the RE application on DIII-D.



Trey Gebhart
Postdoctoral Research Associate

Thermal-Hydraulics Experiments on He-Cooled Solid Divertors



Application

Helium-cooled solid divertors are the leading candidate for solving power and particle exhaust issues in long-pulse fusion magnetic fusion devices

Engineering Achievement

Simulations and initial experiments suggest that the complex He-cooled modular (“finger”) divertor with multiple jets (HEMJ) and simplified finger design have comparable higher heat transfer coefficients

Significance and Impact

Simpler divertor design should improve reliability, reduce cost

Research Details + Schedule

- Ongoing maintenance of current Georgia Tech He loop
 - Test section and RF heater coil enclosed in vacuum chamber
 - Installed flow meters for direct measurements of He mass flow rate through test section
 - Compressor maintenance: replacing valves/seals
- Starting experiments of HEMJ test section and simplified finger design (flat cooled surface with 7 jets): at higher He inlet temperatures $T_i = 300\text{--}425$ °C
- Initial results for nondimensionalized heat transfer coefficient Nu (points) in reasonable agreement with simulations (dashed lines)
- Thermal performance of simplified finger comparable to that of HEMJ

Bailey Zhao, M. Yoda, S. I. Abdel-Khalik, S. Musa

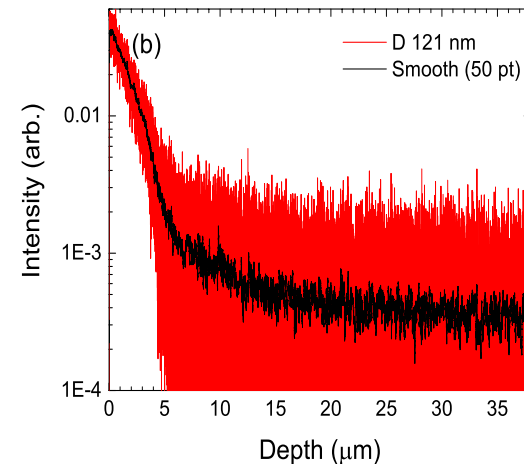


Fresh Faces of VLT
PhD candidate: Bailey Zhao

Glow discharge optical emission spectroscopy

- **Technique**
 - Elemental characterization with depth profiling.
 - Analyzed 10s of elements simultaneously.
 - Nanometer depth resolution.
 - Sputtering rates of $\mu\text{m}/\text{min}$.
- **Specifications**
 - Capable of differentiating H and D.
 - Realtime depth measurements.
 - Monochromator can be used to look at unknown element.
- **GD-OES is capable of measuring the D depth profiling from bulk ($\gg 10\mu\text{m}$) neutron-irradiated tungsten exposed to plasma.**

One of few surface analysis techniques capable of directly measuring hydrogen.



Plotting the smoothed data (50 point averaging) semi-log scale in (b) indicates that smaller quantities of deuterium are found up to $>20\mu\text{m}$ in the sample.



Chase N. Taylor
Early Career Staff



Improved bulk & surface diagnostics at STAR continues to enhance tritium & nuclear PMI sciences

- **Challenge:** Limited availability of bulk and surface diagnostics for neutron-irradiated and tritium contaminated samples.
- **Significance and Impact:** Improvement of bulk and surface diagnostics at STAR facility enables characterizing bulk and surfaces of neutron-irradiated and tritium contaminated samples (for the first time) to advance fusion nuclear sciences and fusion safety [1,2].



X-ray photoelectron spectroscopy (FES funded for relocation/setup)



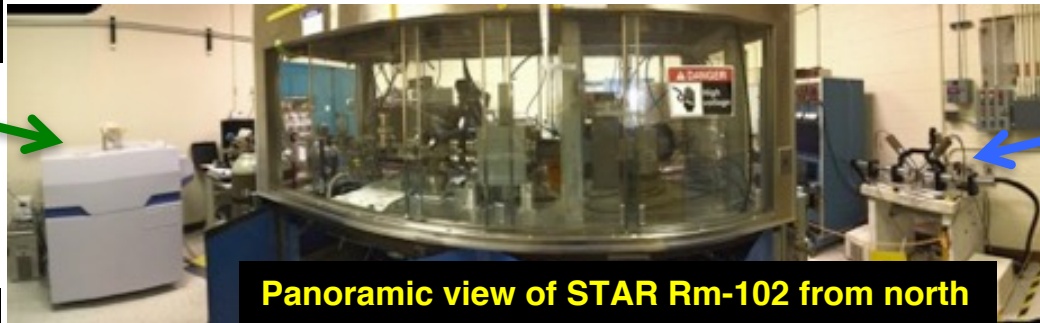
Panoramic view of STAR Rm-102 from southeast corner



Scanning Auger Microscopy (FES funded for relocation/setup)



Glow Discharge Optical Emission Spectrometry (INL funded)



Panoramic view of STAR Rm-102 from north



Coincidence Doppler and Positron Lifetime Spectroscopy (INL funded)

- **STAR Publications in FY17 Q3** [1] M. Shimada, C. N. Taylor, R. J. Pawelko, L. C. Cadwallader & B. J. Merrill, "Tritium Plasma Experiment Upgrade and Improvement of Surface Diagnostic Capabilities at STAR Facility for Enhancing Tritium and Nuclear PMI Sciences", *Fusion Sci. and Technol.* [2] C.N. Taylor and M. Shimada, "Direct depth distribution measurement of deuterium in bulk tungsten exposed to high-flux plasma", *AIP Advance* 7 (2017) 055305

Effects of applied strain on nanoscale self-interstitial cluster formation in BCC iron

Science Objective

Understand the effects of external stress on formation of self-interstitial atom (SIA) clusters in body-centered cubic iron using atomistic simulations

Why it Matters

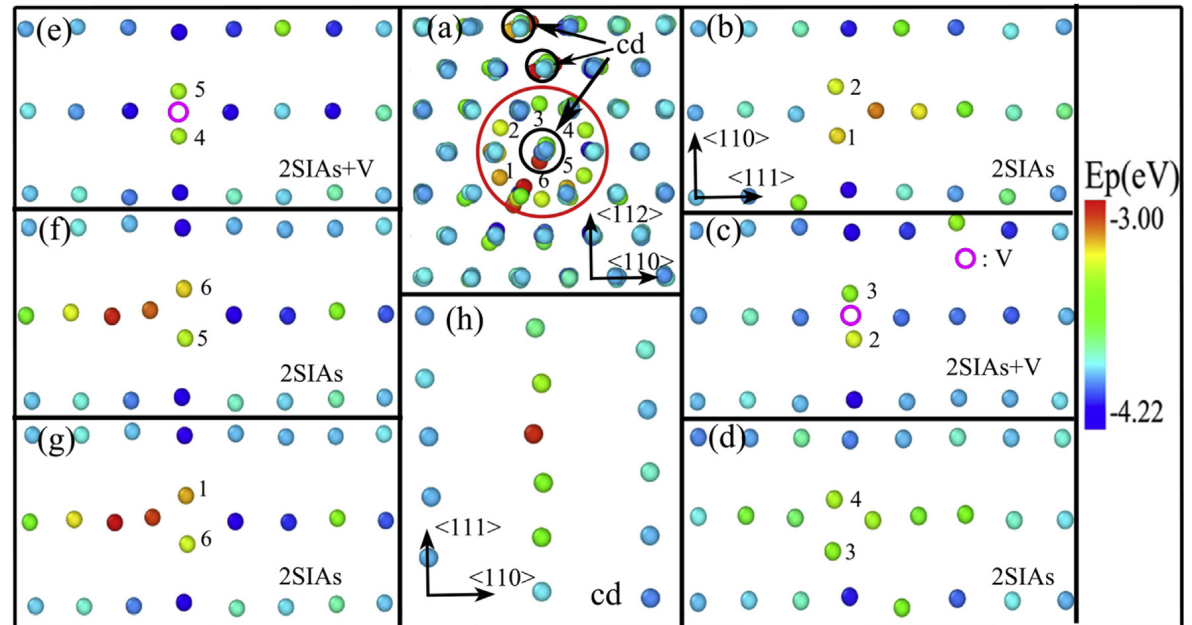
SIAs, vacancies and clusters of these species, form during irradiation of materials, but little is known about the structure of nanoscale SIA clusters, which can influence microstructure evolution. Novel immobile cluster configurations not typically reported in displacement cascade simulations were discovered

Method

The method developed by Monasterio et al. was used to randomly insert SIAs into the simulation box. Up to 7 SIAs were inserted one by one every 40 ps to explore nanocluster evolution

Ning Gao (CAS), Wahyu Setyawan, Rick Kurtz, Zhiguang Wang (CAS), *Journal of Nuclear Materials* 493 (2017) 62.

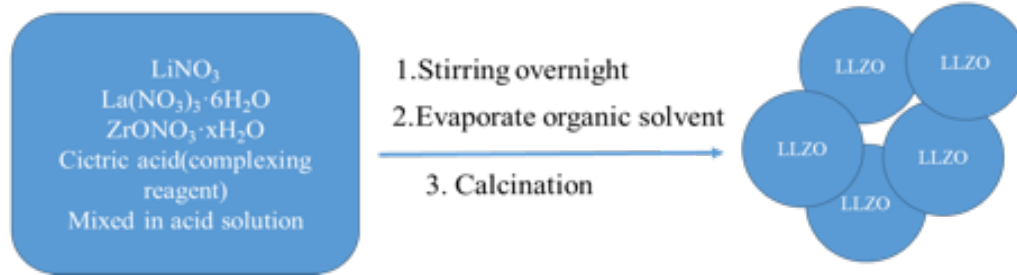
<http://dx.doi.org/10.1016/j.jnucmat.2017.05.044>



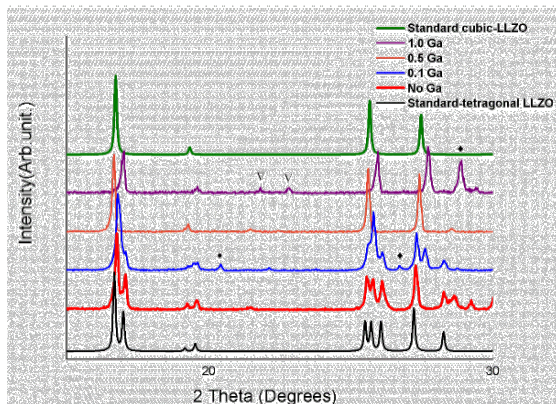
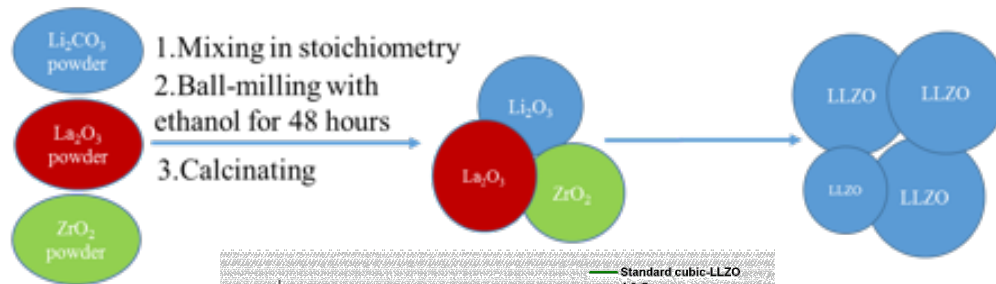
A new SIA cluster configuration consisting of 7 SIAs viewed along a $\langle 111 \rangle$ direction in (a). The new configuration is comprised of three $\langle 111 \rangle$ crowdions and four $\langle 110 \rangle$ dumbbells, namely a central $\langle 111 \rangle$ crowdion surrounded by a ring of four $\langle 110 \rangle$ dumbbells and two additional $\langle 111 \rangle$ crowdions outside the ring. Details of the crowdions and dumbbells are shown in (b) to (h). There are two different $\langle 110 \rangle$ dumbbells with two dumbbell atoms sharing one lattice site or not. The defect in (h) is an example of a $\langle 111 \rangle$ crowdion. Atoms are colored based on their potential energy (E_p)

Demonstration of Direct LiT Electrolysis using an Immersion Cell

- Sol-gel route: $7\text{Li}^+ + 3\text{La}^{3+} + 2\text{Zr}^{4+} + 12\text{O}^{2-} \rightarrow \text{Li}_7\text{La}_3\text{Zr}_2\text{O}_{12}$ (C, N become gas during Calcination)



- SSR route: $7\text{Li}_2\text{CO}_3 + 4\text{ZrO}_2 + 3\text{La}_2\text{O}_3 = 2\text{Li}_7\text{La}_3\text{Zr}_2\text{O}_{12} + 7\text{CO}_2\uparrow$



Scientific Achievement

- Improvement of the conductivity and structural integrity of the solid lithium ion conducting materials is critical to creating a viable direct LiT electrolysis process
- Additives to the solid electrolyte can help to **improve conductivity and strength** the Lithium Lanthanum Zirconate (LLZO)

Significance and Impact

The development of a **sol-gel synthesis method** allows **significant variation of LLZO electrolyte properties** and can be used to **increase conductivity and strength of the electrolyte**

Research Details

- A gallium additive was included into the LLZO synthesis that increases the formation of cubic phase in the electrolyte. The cubic phase has higher Li-ion conductivity than the tetragonal phase

B. Garcia-Diaz, J. A. Teprovich,
H. R. Colon-Mercado

Low power tests of polarizers at 170 GHz for EC heating in ITER

Scientific Achievement

Low power measurements were done on miter-bend polarizers for converting a linearly polarized microwave beam into an arbitrary elliptically polarized beam for Electron Cyclotron Heating in ITER.

Significance and Impact

ECH power, transported through highly oversized corrugated metallic waveguides, must achieve a specific elliptical polarization in order to be launched and absorbed as needed in ITER.

Research Details

- Mode content measurements were performed to analyze the mode conversion in the miter-bend assembly when the grating is rotated to control the polarization (see figure).
- A small amount of mode conversion was observed in the rotator miter-bend assembly.

• Application

These results are critical to designing the ITER ECH transmission lines but also apply to all other ECH experiments.

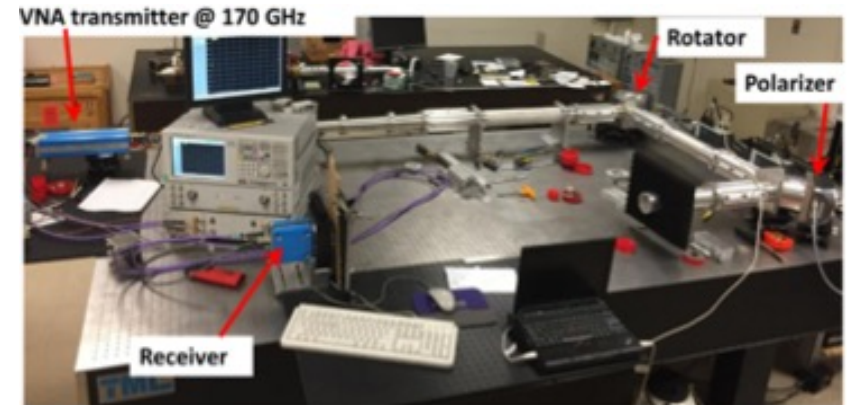
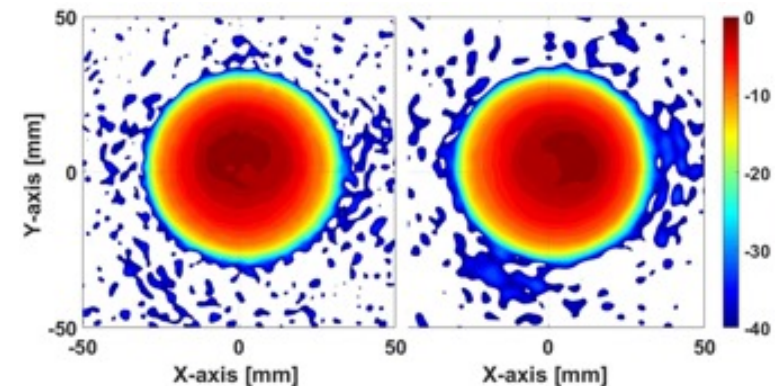


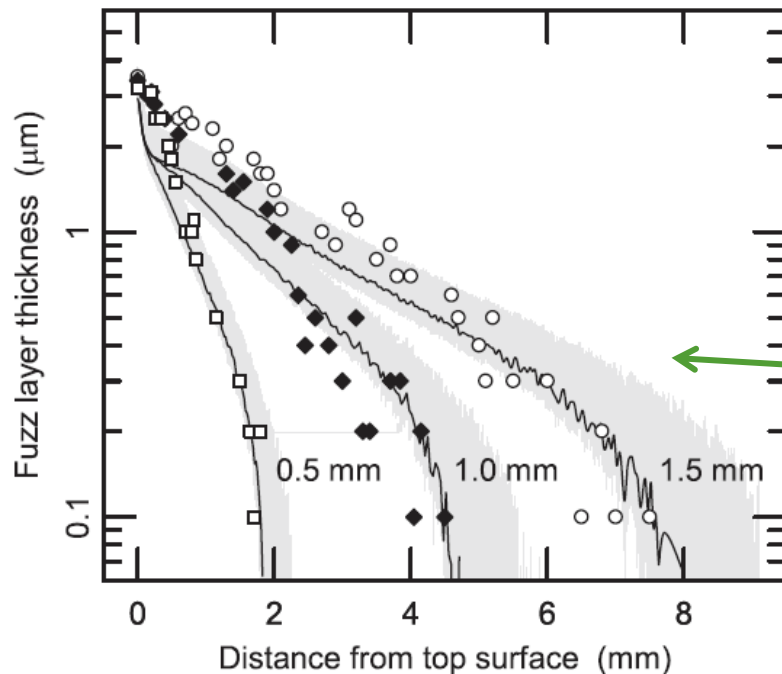
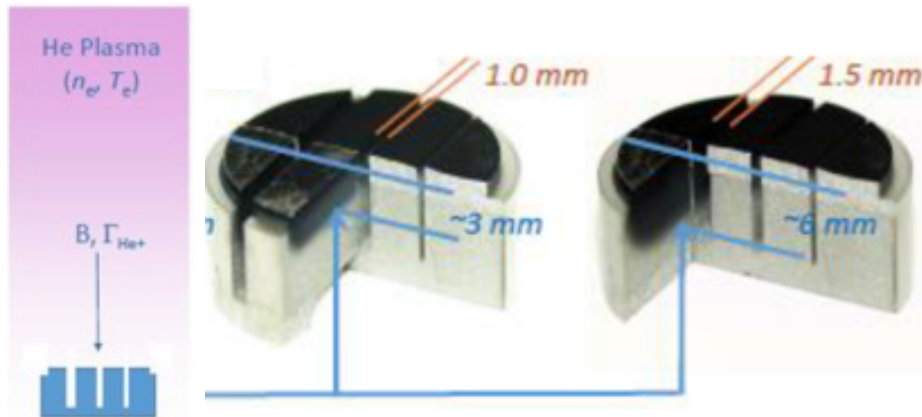
Photo of the test lab.



Measured intensities at the 63.5 mm corrugated waveguide aperture for grating rotation angle of 90° (a) and 270°

MIT: H. Hoffmann, S. Jawla, M. Shapiro and R. Temkin & G. Hanson, ORNL; supported by DOE VLT and US IPO

W fuzz growth used to validate plasma-gap penetration models as part of US-EU Bilateral Collaboration on PMI



- Fuzz growth is observed on the sidewalls of castellated W targets exposed to He plasma in PISCES
- Models predict fuzz growth depends of He fluence
 - [T.Petty et al. NF 55 \(2015\)093033\]](#)
- Particle-in-cell (PIC) model developed at Czech Academy of Science is used to predict sidewall He flux with differing gap width
- Measurements (symbols) and model (lines, shaded area represent uncertainty) agree as gap width varies

[M.J. Baldwin](#), [R. Dejarnac](#), [M. Komm](#) and [R.P. Doerner](#),
 Plasma Physics and Control. *Fusion* 59(2017)064006

Modeling SOL plasma/neutral interactions with PFCs in present-day devices validates models

Scientific Objective

Develop and validate simulation models of particle and heat fluxes to plasma-facing components (PFCs) on present-day devices and assess innovative divertor designs. Aid physics understanding of data.

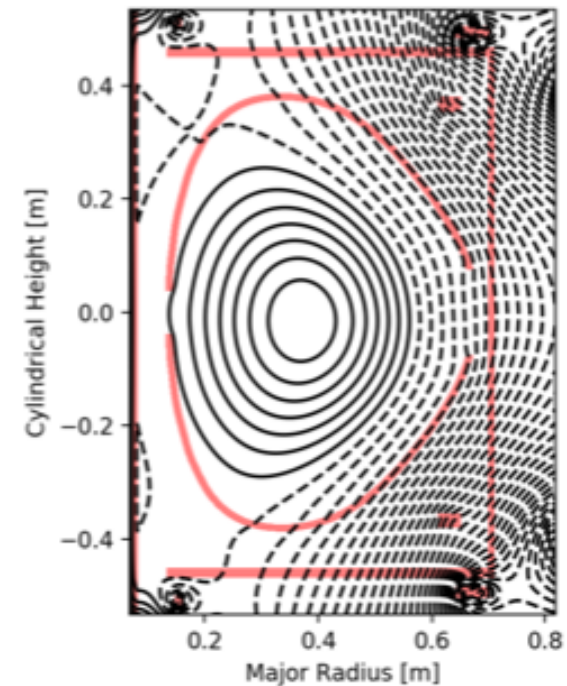
Achievement

- PPCF joint publication accepted: compares UEDGE/TCV-data on effects of ExB/magnetic drifts on PFC heat flux. Trends ok, details need work.
- Initiated work with LTX researchers to perform 4D kinetic simulations of hot, low density scrape-off layer using COGENT. A test-version of an LTX-like geometry suitable for COGENT simulations has been constructed, and first simulations performed.
- Continued support of snowflake divertor simulations for present-day devices including cross-field drifts.

Why it matters

Predictive capability of particle and power loads on PFCs is very important to guiding safe and economical operation of high-power devices such as ITER and to design of future devices.

Magnetic flux-surface structure for LTX experiments being implemented in the COGENT kinetic edge code



Courtesy Chris Hansen, UW

N. Christen, C. Theiler, T.D. Rognlien et al., *Plasma Phys. Contr. Fusion*, accepted.

Critical issues for liquid PFCs include managing power & particle fluxes and shielding vapor

Scientific Objective

Predict edge-plasma properties and divertor geometries that are integrated with core plasma operation and the characteristics of liquid walls for an FNSF design. Compare results with similar configurations that used solid walls to identify key issues and impact on overall fusion performance.

Achievement

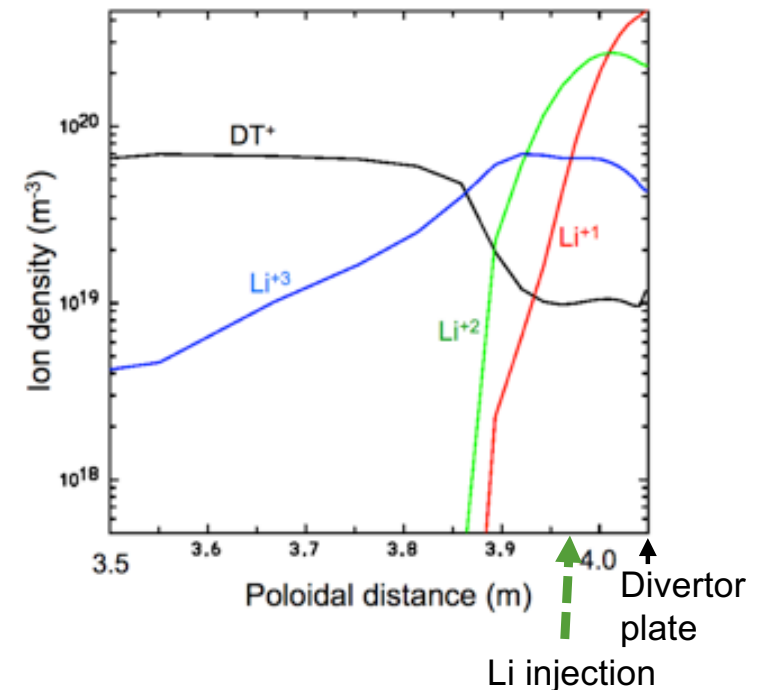
Performed 1D and 2D UEDGE simulations of possible lithium divertor for FNSF; initial model mimics Li evaporation by injected gas source

Results show that a stable plasma configuration can form with Li dominating over DT near the divertor plate. At least 60% of the input power can be radiated by Li. Electron temperatures of ~5 eV achieved, Detached plasma operation requires improved model for Li source.

Why it matters

Flowing liquid walls could avoid the issue of wall erosion by ions and neutrals and could also lead to high-performance core operational modes.

Ion densities in the divertor region of FNSF modeled by UEDGE assuming strong influx of lithium from plate region



T.D. Rognlien, M.E. Rensink, *Fusion Eng. Design*, submitted.

Toward high-field compact fusion magnets: Understand the bending strain in REBCO conductors to optimize cable and magnet design with minimum conductor degradation

Scientific Achievement

Developed a curvature-based numerical method to determine the strain distribution in the brittle REBCO layer of coated conductors.

Significance and Impact

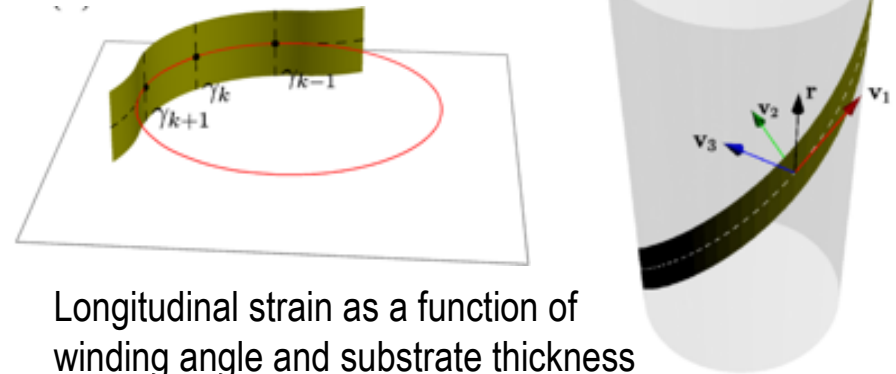
REBCO tapes are promising for high-field compact fusion reactor magnets. The tapes cannot be arbitrarily bent which poses a significant challenge for cable and magnet design as excessive strain can degrade the conductor. The developed approach allows to optimize the REBCO cable and magnet design to minimize the conductor strain.

Research Details

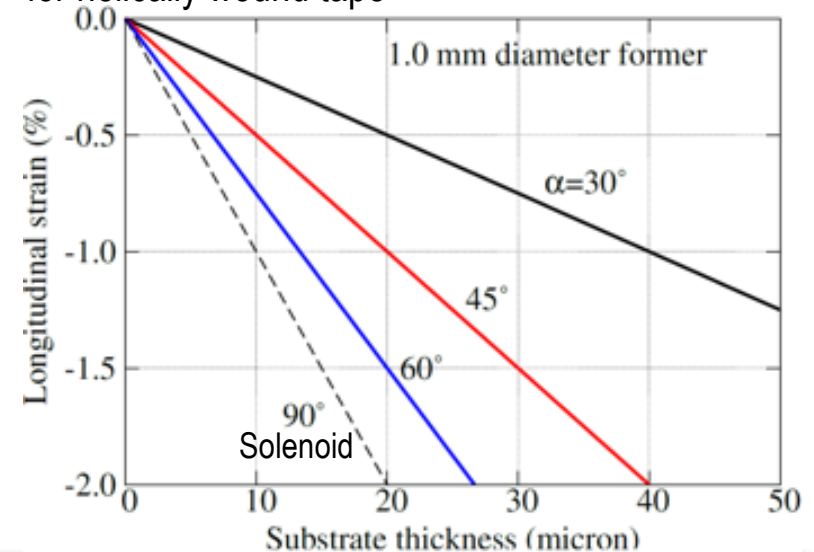
The local curvature of tapes bent with the constant-perimeter method (rectifying developable surface) are determined. Two orthogonal strain components are determined: the longitudinal strain along the conductor length and the transverse strain along the conductor width.

“Strain Distribution in REBCO Coated Conductors Bent with the Constant-Perimeter Geometry”, X. Wang, D. Arbelaez, S. Caspi, S. O. Prestemon, G.L. Sabbi, T. Shen, submitted to IEEE Transactions on Applied Superconductivity

Local curvature defined by osculating circles

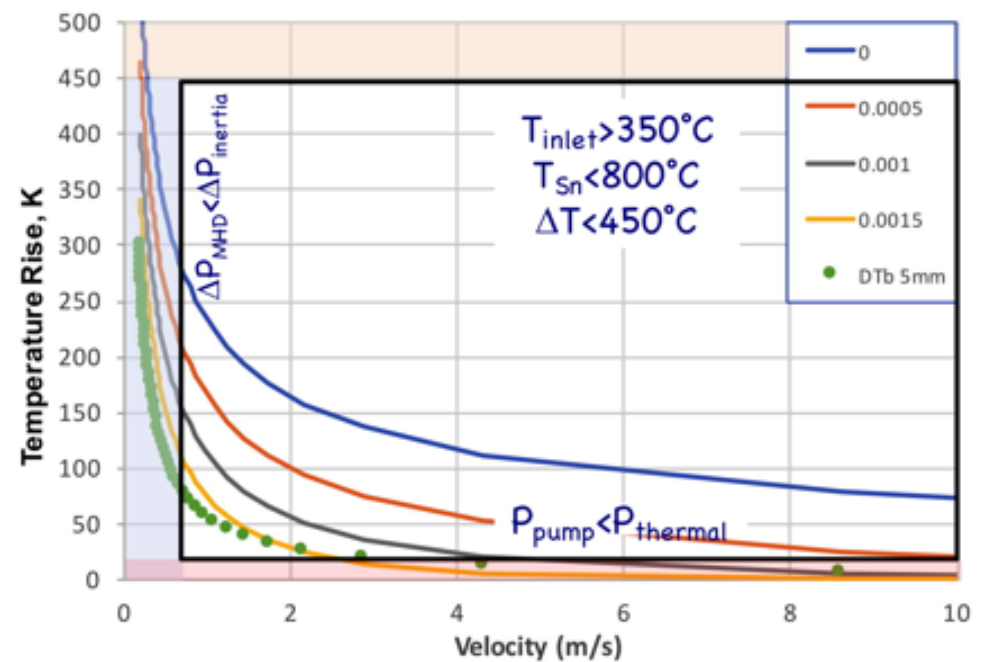
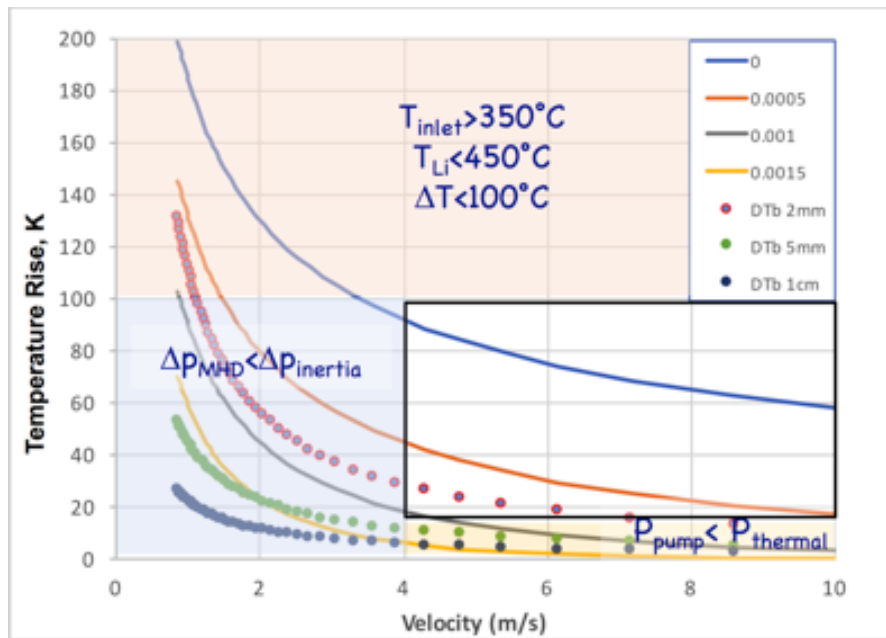


Longitudinal strain as a function of winding angle and substrate thickness for helically wound tape



FESS: Liquid metal PFC study exploring LM features, substrates and FW/divertor concepts

Thermohydraulic analys: Li and Sn temperature range, pumping power, thermal conversion, flow speed & losses operating space



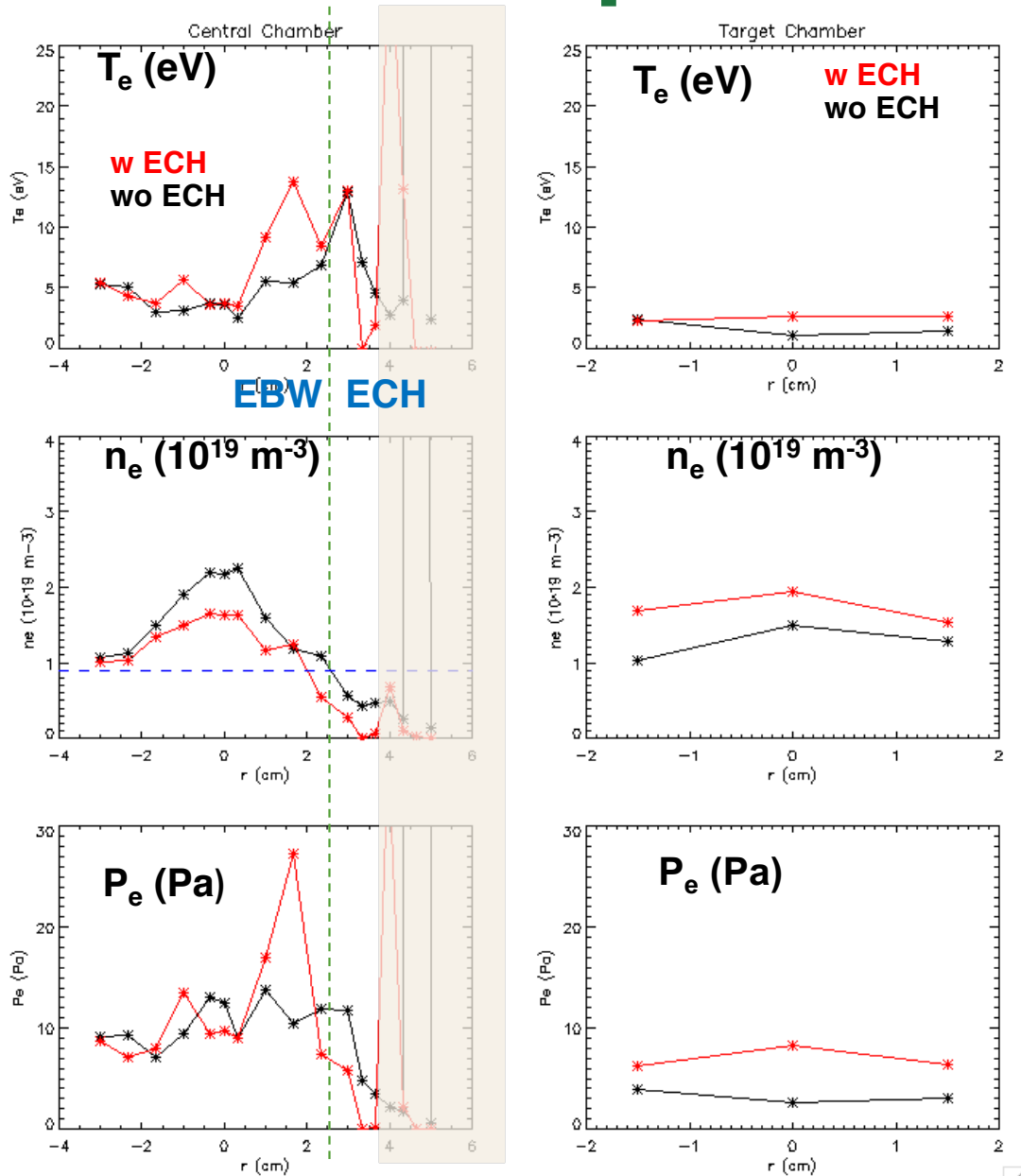
Lithium probably requires both in-situ pumping and evaporation suppression to operate at a tolerable velocity

Tin allows a large DT_{bulk} (50°C) and can support a free-streaming film without in-situ pumping

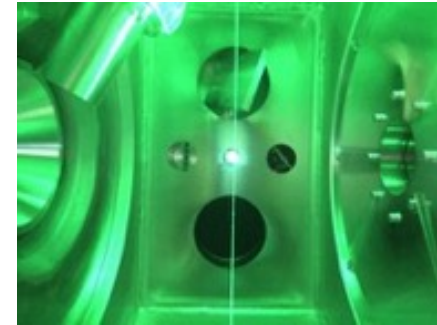
M. Tillack (UCSD)



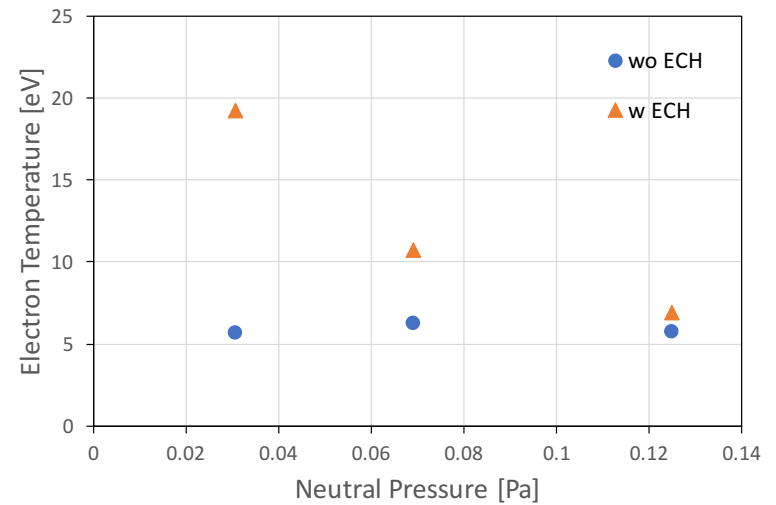
Electron heating has been confirmed on Proto-MPEX as predicted



New Thomson Scattering beam line in central chamber allows to determine heating physics better

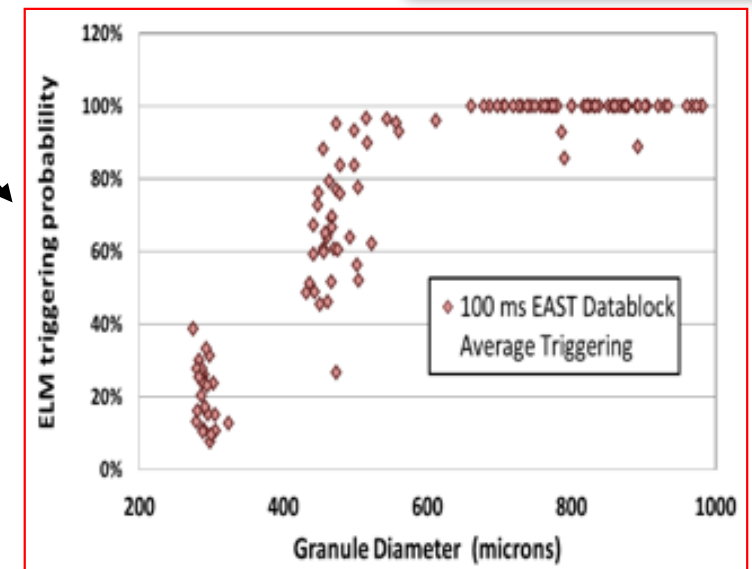
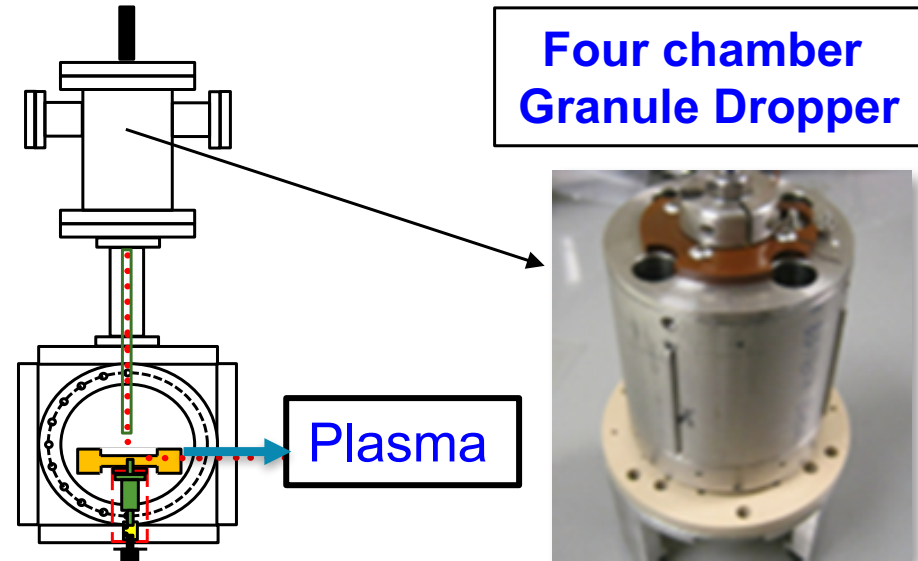


Electron heating considerably stronger at lower neutral pressure as predicted.



Four chamber lithium granule injector used in EAST to determine ELM triggering efficiency vs size

- ELM triggering assessed in discharges with 6.5 MW P_{aux}
 - ELM triggering probability $\sim 100\%$ for Li granules > 0.5 mm in EAST, drops off rapidly below that size (R. Lunsford, EPS 2017)
 - Size threshold similar to that measured in DIII-D with LGI (A. Bortolon, NF 2016)
 - ELM pacing also demonstrated in discharges using the upper W divertor
- Next step: use discharges with low ELM frequency to determine if q_{peak} and $E_{peak} \sim 1/f_{ELM}$



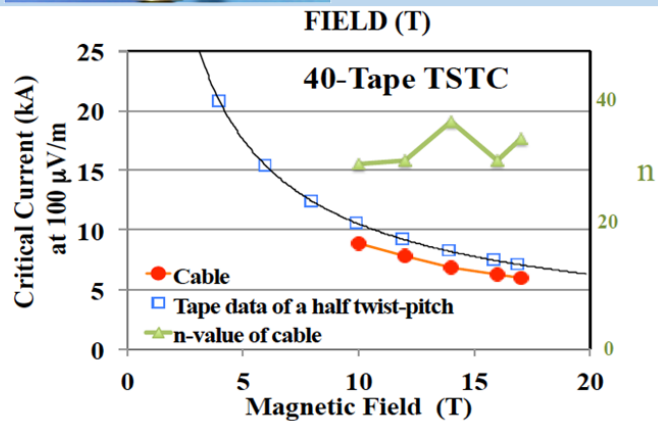
Electromechanical characteristics of high current, high field conductors using REBCO HTS tapes

REBCO TSTC Small Coiled Sample Tested at NHMFL

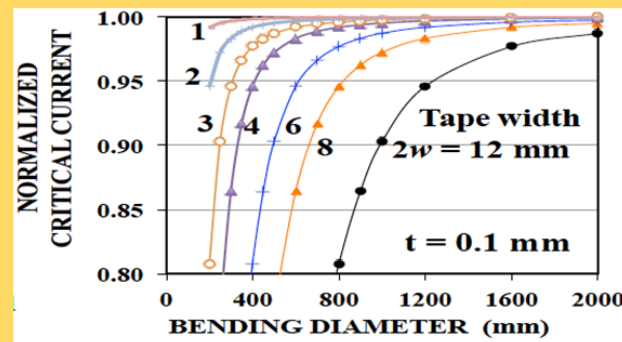
- 40-Tape, 2.6 Turn, 2.6 m cable wound with about 200 mm twist-pitch on pentagon shaped cylinder surface. (REBCO tape: SuperPower 4 mm width, 0.1 mm thick, 120 A at 77 K)
- Tested at NHMFL using 17 T, 195 mm warm-bore Bitter magnet.
- Fabricated using Stacked-Tape Twist-Wind (STTW) method.



- No cyclic load effect (102 kN/m)
- Compared to single tape data the degradation was 16%.
- J_e (6 kA at 17 T) = 375 A/mm²

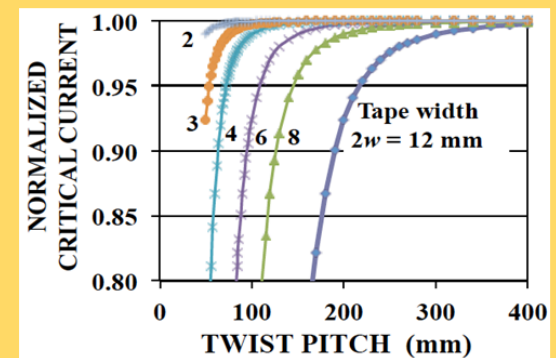


Bending Characteristic of TSTC



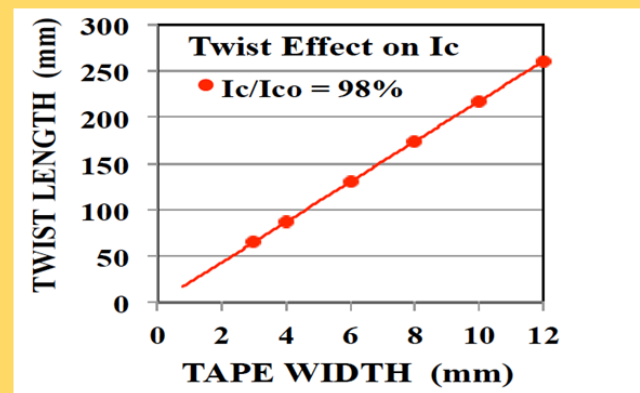
I_c degradation due to bending based on Perfect-Slip Model

Twisting Characteristic of TSTC

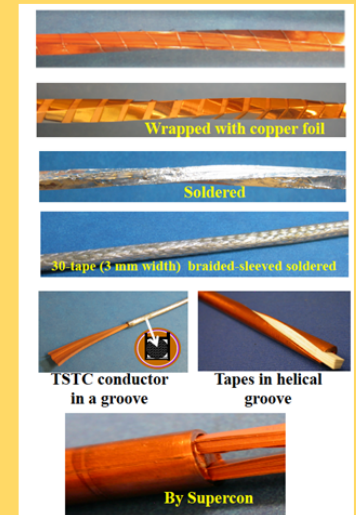


I_c degradation due to twisting

Twist Length vs. Tape Width



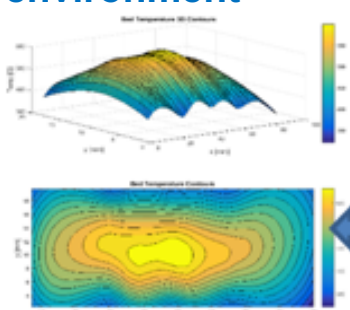
Critical Twist-Pitch \approx 22 times Tape-Width



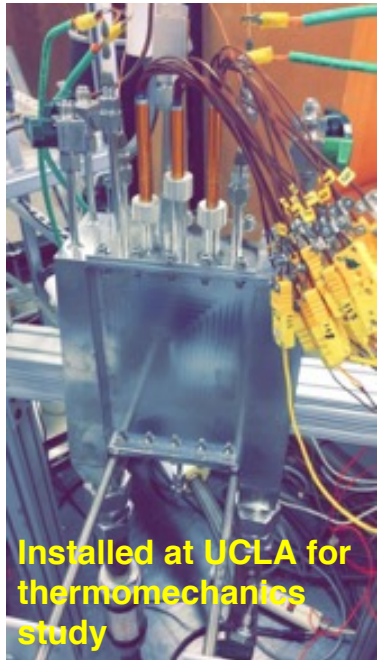
UCLA FUSION SCIENCE and TECHNOLOGY CENTER

Focused R&D in niche areas of US scientific strength, capability, and leadership on FNS and Materials Interactions/Blanket/Tritium

Ceramic Breeder/Structural Material System Thermomechanics - US/UCLA-KO/NFRI Collaboration: Investigation of ceramic breeder pebble bed/structural material system thermomechanics with volumetric heating and temperature gradient representative of the fusion nuclear environment



Measured temperature profile in a Li_2TiO_3 pebble bed simulated by wire heater block in a preliminary test article at UCLA



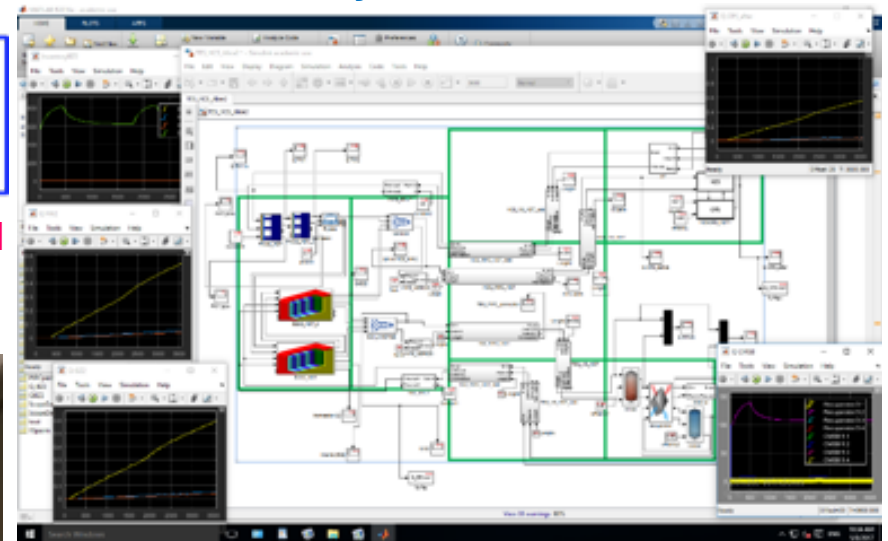
Installed at UCLA for thermomechanics study

Test article (TESOMEX) fabricated at KAERI using Korean ARAA reduced ferritic steel



Mahmoud Lotfy, Alice Ying, Mohamed Abdou, Yi-Hyun Park, Seungyon Cho, Study on the Thermally-Induced Stress and Relaxation of Ceramic Breeder Pebble Beds, Published online: 19 Jun 2017, FS&T

Matlab-Simulink/COMSOL Tritium Dynamic Modeling Development for HCCR TBS - UCLA-NFRI-INL Phase 2 Collaboration In support of HCCR Preliminary Design Review, accurate dynamic tritium permeation data in port interspace/port cell, vertical shaft are needed as part of the design/safety/maintenance analysis.



Hongjie Zhang, Alice Ying, Mohamed Abdou, Masashi Shimada, Bob Pawelko, Seungyon Cho, Characterization of Tritium Isotopic Permeation Through ARAA in Diffusion Limited and Surface Limited Regimes, Published online: 22 Jun 2017, FS&T

Christopher Kang, Yi-Hyun Park, Jon T. Van Lew, Alice Ying, Mohamed Abdou, Seungyon Cho, Transient Hot-Wire Experimental System for Measuring the Effective Thermal Conductivity of a Ceramic Breeder Pebble Bed, Published online: 30 Jun 2017, FS&T

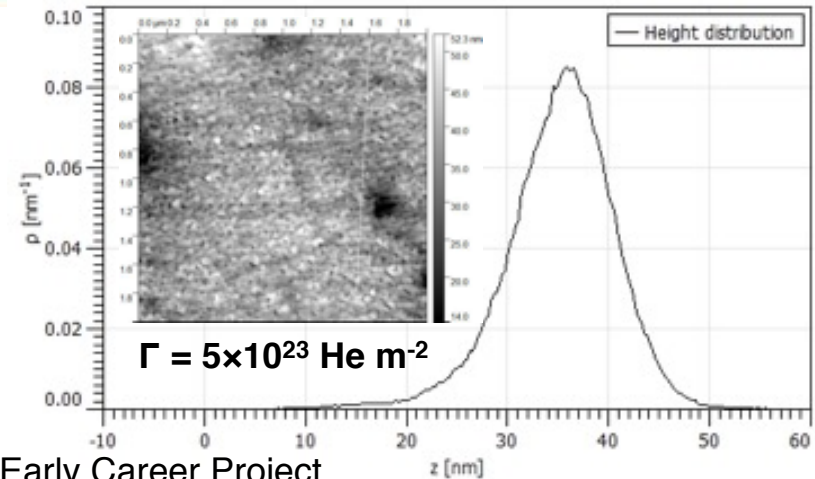
Science based understanding of PSI

- How do high fluxes of H/D/T and He interact with materials? (*TPE & PISCES collaborations*)

Helium bubble layer in PISCES samples examined by ellipsometry
Hydrogen retention in UFG tungsten using DiMES on DIII-D

- What is the dynamic response of surfaces? (*UT & PISCES collaborations*)

AFM / He ion microscopy of early stages of W fuzz formation compared with continuum model simulations by Brian Wirth



DOE Early Career Project
Robert Kolasinski

Improved plasma edge measurements

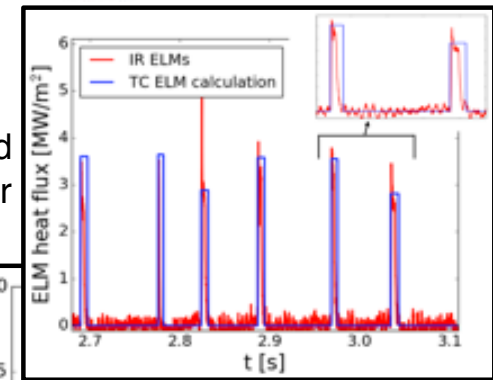
- Measure erosion/redeposition accurately (*DIII-D, NSTX-U, EAST collaborations*)

W coated DiMES characterized by RBS to calibrate real-time erosion

- SAS divertor probes, embedded TCs, H-sensors

Embedded thermocouples and Langmuir probes used to determine inter- and intra ELM energy deposition (Postdoc: Joseph Barton, PFMC16 paper)

Diagnostics needed for the SAS divertor



Science-based engineering

- PFC thermal models help us understand power handling and how PFCs fail. (*DIII-D, NSTX-U*)

New thermal analysis to model ELM heat load to tungsten leading edges

- Developing novel materials and designs

Li-Ta heat pipe development with Thermacore. Additive manufacturing for refractories.

